

# What can we learn about GW Physics with an elastic spherical antenna?

J. Alberto Lobo

*Departament de Física Fonamental  
Universitat de Barcelona, Spain.*

(5 December 1994)

(Revised October 30, 2018)

A general formalism is set up to analyse the response of an *arbitrary* solid elastic body to an *arbitrary metric* Gravitational Wave perturbation, which fully displays the details of the interaction antenna-wave. The formalism is applied to the spherical detector, whose sensitivity parameters are thereby scrutinised. A *multimode* transfer function is defined to study the amplitude sensitivity, and absorption cross sections are calculated for a general metric theory of GW physics. Their *scaling* properties are shown to be *independent* of the underlying theory, with interesting consequences for future detector design. The GW incidence direction deconvolution problem is also discussed, always within the context of a general metric theory of the gravitational field.

04.80.Nn, 95.55.Ym

## I. INTRODUCTION

The idea of building ultracryogenic spherical Gravitational Wave (GW) antennae seems to be progressively winning adepts, even despite the technological difficulties of various kinds posed by a project like that, which every expert acknowledges. Confidence in its feasibility stems from many years of experience: groups at Stanford, Louisiana State University, Roma and Legnaro (Italy) and Perth (Western Australia) have constructed and operated, at different levels, cryogenic cylindrical bars of the Weber type [1]. In particular, a *long term* strain sensitivity  $h = 6 \times 10^{-19}$  for millisecond bursts has been reported from the bar *EXPLORER* [2]. The new generation ultracryogenic cylinder *NAUTILUS*, of the Frascati group [3], is beginning operation as these lines are written [4], with an expected sensitivity nearly an order of magnitude better than the above.

Spherical antennae are considered by many to be the natural next step in the development of resonant GW detectors [5–10]. The reasons for this new trend essentially derive from the *improved sensitivity* of a sphere —which can be nearly an order of magnitude better than a cylinder having the same resonance frequency, see below and [10]—, and from its *multimode capabilities*, first recognised by Forward [5] and further elaborated in [7,8].

Although some of the most relevant aspects of detector sensitivity have already received attention in the literature, it seems to me that a sufficiently general and flexible analysis of the interaction detector-GW has not been satisfactorily developed to date. This *theoretical* shortage has a number of *practical* negative consequences, too. Traditional analysis, to mention but an example, is almost invariably restricted to General Relativity or scalar–tensor theories of gravity; while it may be argued that this is already very general, any such argument is, as a matter of fact, understating the potentialities actually offered by a spherical GW antenna to help decide for or against any one specific theory of the gravitational field on the basis of *experimental observation*.

I thus propose to develop in this paper a full fledged mathematical formalism which will enable analysis of the antenna’s response to a completely general GW, i.e., making no *a priori* assumptions about which is the correct theory underlying GW physics (other than, indeed, that it is a *metric* theory), *and* also making no assumptions about detector shape, structure or boundary conditions. Considering things in such generality is not only “theoretically nice” —it also brings about new results and a *better understanding* of older ones. For example, it will be proved that the sphere is the *most efficient* GW elastic detector shape, and that higher mode absorption cross sections *scale independently of GW physics*. I will also discuss the direction of incidence deconvolution problem in the context of a general metric theory of gravity.

The paper is organised as follows: section 2 is devoted to the development of the general mathematical framework, leading to a formula in which an elastic solid’s response is related to the action of an arbitrary metric GW impinging on it. In section 3 the general equations are applied to the homogeneous spherical body, and a discussion of the *deconvolution* problem is presented as well. Section 4 contains the description of the sphere’s sensitivity parameters, specifically leading to the concept of *multimode*, or vector, *transfer function*, and to an analysis of the *absorption cross section* presented by this detector to a passing by GW. Conclusions and prospects are summarised in section 5, and two appendices are added which include mathematical derivations.

## II. GENERAL MATHEMATICAL FRAMEWORK

In the mathematical model, I shall be assuming that the antenna is a solid elastic body which responds to GW perturbations according to the equations of classical non-relativistic linear Elasticity Theory [11]. This is fully justified since, as stressed above, GW induced displacements will be very small indeed, and the speed of such displacements much smaller than that of light for any foreseeable frequencies. Although our primary interest is a spherical antenna, the considerations which follow in the remainder of this section *have general validity for arbitrarily shaped isotropic elastic solids*.

Let  $\mathbf{u}(\mathbf{x}, t)$  be the displacement vector of the infinitesimal mass element sitting at point  $\mathbf{x}$  relative to the solid's centre of mass in its unperturbed state, whose density distribution in that state is  $\rho(\mathbf{x})$ . Let  $\lambda$  and  $\mu$  be the material's elastic Lamé coefficients. If a volume force density  $\mathbf{f}(\mathbf{x}, t)$  acts on such solid, the displacement field  $\mathbf{u}(\mathbf{x}, t)$  is the solution to the system of partial differential equations [11]

$$\rho \frac{\partial^2 \mathbf{u}}{\partial t^2} - \mu \nabla^2 \mathbf{u} - (\lambda + \mu) \nabla(\nabla \cdot \mathbf{u}) = \mathbf{f}(\mathbf{x}, t) \quad (2.1)$$

with the appropriate initial and boundary conditions. A summary of notation and general results regarding the solution to that system is briefly outlined in the ensuing subsection, as they are necessary for the subsequent developments in this paper, and also in future work.

### A. Separable driving force

For reasons which will become clear later on, we shall only be interested in driving forces of the separable type

$$\mathbf{f}(\mathbf{x}, t) = \mathbf{f}(\mathbf{x}) g(t) \quad (2.2)$$

or, indeed, linear combinations thereof. The solution to (2.1) does not require us to specify the precise boundary conditions on  $\mathbf{u}(\mathbf{x}, t)$  at this stage, but we need to set the initial conditions. We adopt the following:

$$\mathbf{u}(\mathbf{x}, 0) = \dot{\mathbf{u}}(\mathbf{x}, 0) = 0 \quad (2.3)$$

where  $\dot{\cdot} \equiv \partial/\partial t$ , implying that the antenna is at complete rest before observation begins at  $t=0$ . The structure of the force field (2.2) is such that the displacements  $\mathbf{u}(\mathbf{x}, t)$  can be expressed by means of a *Green function* integral of the form

$$\mathbf{u}(\mathbf{x}, t) = \int_0^\infty \mathbf{S}(\mathbf{x}; t - t') g(t') dt' \quad (2.4)$$

The deductive procedure whereby  $\mathbf{S}(\mathbf{x}; t - t')$  is calculated can be found in many standard textbooks —see e.g. [12]. The result is

$$\mathbf{S}(\mathbf{x}; t) = \begin{cases} 0 & \text{if } t \leq 0 \\ \sum_N \frac{f_N}{\omega_N} \mathbf{u}_N(\mathbf{x}) \sin \omega_N t & \text{if } t \geq 0 \end{cases} \quad (2.5)$$

where

$$f_N \equiv \frac{1}{M} \int_{\text{Solid}} \mathbf{u}_N^*(\mathbf{x}) \cdot \mathbf{f}(\mathbf{x}) d^3x \quad (2.6)$$

and  $\mathbf{u}_N(\mathbf{x})$  are the normalised *eigen-solutions* to

$$\mu \nabla^2 \mathbf{u}_N + (\lambda + \mu) \nabla(\nabla \cdot \mathbf{u}_N) = -\omega_N^2 \rho \mathbf{u}_N \quad (2.7)$$

with suitable *boundary conditions*. Here  $N$  represents an index, or set of indices, labelling the *eigenmode* of frequency  $\omega_N$ . The normalisation condition is (arbitrarily) chosen so that

$$\int_{\text{Solid}} \mathbf{u}_{N'}^*(\mathbf{x}) \cdot \mathbf{u}_N(\mathbf{x}) \rho(\mathbf{x}) d^3x = M \delta_{N'N} \quad (2.8)$$

where  $M$  is the total mass of the solid, and the asterisk denotes complex conjugation. Replacing now (2.5) into (2.4) we can write the solution to our problem as a series expansion:

$$\mathbf{u}(\mathbf{x}, t) = \sum_N \frac{f_N}{\omega_N} \mathbf{u}_N(\mathbf{x}) g_N(t) \quad (2.9)$$

where

$$g_N(t) \equiv \int_0^t g(t') \sin \omega_N(t - t') dt' \quad (2.10)$$

Equation (2.9) is the *formal* solution to our problem; it has the standard form of an orthogonal expansion and is valid for *any* solid driven by a separable force like (2.2) and *any* boundary conditions. It is therefore *completely general*, given that type of force.

Before we go on, it is perhaps interesting to quote a simple but useful example. It is the case of a solid hit by a *hammer blow*, i.e., receiving a sudden stroke at a point on its surface. Exam of the response of a GW antenna to such perturbation is being used for correct tuning and monitoring of the device [13]. If the driving force density is represented by the simple model

$$\mathbf{f}^{(\text{hb})}(\mathbf{x}, t) = \mathbf{f}_0 \delta^{(3)}(\mathbf{x} - \mathbf{x}_0) \delta(t) \quad (2.11)$$

where  $\mathbf{x}_0$  is the surface point hit, and  $\mathbf{f}_0$  is a constant vector, then the system's response is immediately seen to be

$$\mathbf{u}^{(\text{hb})}(\mathbf{x}, t) = \sum_N \frac{f_N^0}{\omega_N} \mathbf{u}_N(\mathbf{x}) \sin \omega_N t \quad (2.12)$$

with  $f_N^0 = M^{-1} \mathbf{f}_0 \cdot \mathbf{u}_N^*(\mathbf{x}_0)$ . A hammer blow thus excites *all* the solid's normal modes, except those *perpendicular* to  $\mathbf{f}_0$ , with amplitudes which are *inversely proportional to the mode's frequency*. This is seen to be a rather general result in the theory of sound waves in isotropic elastic solids.

## B. The GW tidal forces

An incoming GW manifests itself as a *tidal* force density; in the long wavelength linear approximation [14] it only depends on the “electric” components of the Riemann tensor:

$$f_i(\mathbf{x}, t) = \rho c^2 R_{0i0j}(t) x_j \quad (2.13)$$

where  $c$  is the speed of light, and sum over the repeated index  $j$  is understood. In (2.13) tidal forces are referred to the antenna's centre of mass, and thus  $\mathbf{x}$  is a vector originating there. Note that I have omitted any dependence of  $R_{0i0j}$  on spatial coordinates, since it only needs to be evaluated at the solid's centre. The Riemann tensor is only required to first order at this stage [15]:

$$R_{0i0j} = \frac{1}{2} (h_{ij,00} - h_{0i,0j} - h_{0j,0i} + h_{00,ij}) \quad (2.14)$$

where  $h_{\mu\nu}$  are the perturbations to flat geometry<sup>1</sup>, always at the centre of mass of the detector.

The form (2.13) is seen to be a sum of three terms like (2.2) —but this three term “straightforward” splitting is not the most convenient, due to lack of invariance and symmetry. A better choice is now outlined.

An *arbitrary symmetric* tensor  $\mathcal{S}_{ij}$  admits the following decomposition:

$$\mathcal{S}_{ij}(t) = \mathcal{S}^{(S)}(t) E_{ij}^{(S)} + \sum_{m=-2}^2 \mathcal{S}^{(m)}(t) E_{ij}^{(m)} \quad (2.15)$$

---

<sup>1</sup> Throughout this paper, *greek* indices ( $\mu, \nu, \dots$ ) will run through space-time values 0,1,2,3; *latin* indices ( $i, j, \dots$ ) will run through space values 1,2,3 only.

where  $E_{ij}^{(m)}$  are 5 linearly independent *symmetric* and *traceless* tensors, and  $E_{ij}^{(S)}$  is a multiple of the *unit* tensor  $\delta_{ij}$ .  $\mathcal{S}^{(S)}(t)$  and  $\mathcal{S}^{(m)}(t)$  are uniquely defined functions, whose explicit form depends on the particular representation of the  $E$ -matrices chosen. A convenient one is the following:

$$E_{ij}^{(S)} = \left(\frac{1}{4\pi}\right)^{\frac{1}{2}} \begin{pmatrix} 1 & 0 & 0 \\ 0 & 1 & 0 \\ 0 & 0 & 1 \end{pmatrix} \quad (2.16a)$$

$$E_{ij}^{(0)} = \left(\frac{5}{16\pi}\right)^{\frac{1}{2}} \begin{pmatrix} -1 & 0 & 0 \\ 0 & -1 & 0 \\ 0 & 0 & 2 \end{pmatrix}, \quad E_{ij}^{(\pm 1)} = \left(\frac{15}{32\pi}\right)^{\frac{1}{2}} \begin{pmatrix} 0 & 0 & \mp 1 \\ 0 & 0 & -i \\ \mp 1 & -i & 0 \end{pmatrix}, \quad E_{ij}^{(\pm 2)} = \left(\frac{15}{32\pi}\right)^{\frac{1}{2}} \begin{pmatrix} 1 & \pm i & 0 \\ \pm i & -1 & 0 \\ 0 & 0 & 0 \end{pmatrix} \quad (2.16b)$$

The excellence of this representation stems from its ability to display the *spin features* of the driving terms in (2.13). Such features are characterised by the relations

$$E_{ij}^{(S)} n_i n_j = Y_{00}(\theta, \varphi), \quad E_{ij}^{(m)} n_i n_j = Y_{2m}(\theta, \varphi) \quad (2.17)$$

where  $\mathbf{n} \equiv \mathbf{x}/|\mathbf{x}|$  is the radial unit vector, and  $Y_{lm}(\theta, \varphi)$  are spherical harmonics [16]. Details about the above  $E$ -matrices are given in Appendix A. In particular, the orthogonality relations (A6) can be used to invert (2.15):

$$\mathcal{S}^{(S)}(t) = \frac{4\pi}{3} E_{ij}^{(S)} \mathcal{S}_{ij}(t) \quad (2.18a)$$

$$\mathcal{S}^{(m)}(t) = \frac{8\pi}{15} E_{ij}^{*(m)} \mathcal{S}_{ij}(t), \quad m = -2, \dots, 2 \quad (2.18b)$$

where an asterisk denotes complex conjugation. Note that  $\mathcal{S}^{(S)}(t) = \sqrt{4\pi} \mathcal{S}(t)/3$ , where  $\mathcal{S}(t) \equiv \delta_{ij} \mathcal{S}_{ij}(t)$  is the tensor's trace.

We now take advantage of (2.15) to express the GW tidal force (2.13) as a sum of split terms like (2.2):

$$\mathbf{f}(\mathbf{x}, t) = \mathbf{f}^{(S)}(\mathbf{x}) g^{(S)}(t) + \sum_{m=-2}^2 \mathbf{f}^{(m)}(\mathbf{x}) g^{(m)}(t) \quad (2.19)$$

with

$$f_i^{(S)}(\mathbf{x}) = \rho E_{ij}^{(S)} x_j, \quad g^{(S)}(t) = \frac{4\pi}{3} E_{ij}^{*(S)} R_{0i0j}(t) c^2 \quad (2.20a)$$

$$f_i^{(m)}(\mathbf{x}) = \rho E_{ij}^{(m)} x_j, \quad g^{(m)}(t) = \frac{8\pi}{15} E_{ij}^{*(m)} R_{0i0j}(t) c^2 \quad (m = -2, \dots, 2) \quad (2.20b)$$

Straightforward application of (2.9) yields the formal solution of the antenna response to a GW perturbation:

$$\mathbf{u}(\mathbf{x}, t) = \sum_N \omega_N^{-1} \mathbf{u}_N(\mathbf{x}) \left[ f_N^{(S)} g_N^{(S)}(t) + \sum_{m=-2}^2 f_N^{(m)} g_N^{(m)}(t) \right] \quad (2.21)$$

with the notation of (2.6) and (2.10) applied *mutatis mutandi* to the terms in (2.20).

Equation (2.21) gives the response of an arbitrary elastic solid to an incoming weak GW, *independently of the underlying gravity theory*, be it General Relativity (GR) or indeed any other *metric* theory of the gravitational interaction. It is also valid for *any antenna shape* and *any boundary conditions*, thus giving the formalism, in particular, the capability of being used to study the response of a detector which is *suspended* by means of a mechanical device in the laboratory site—a situation of much practical importance. It is therefore *very* general.

Equation (2.21) also tells us that that only *monopole* and *quadrupole detector modes* can possibly be excited by a metric GW. The nice thing about (2.21) is that it *fully* displays the monopole-quadrupole *structure* of the solution to our fundamental differential equations.

In a non-symmetric body, all (or *nearly* all) the modes have monopole and quadrupole moments, and (2.21) precisely shows how much each of them contributes to the detector's response. A *homogeneous spherical* antenna, which is very symmetric, has a set of vibrational eigenmodes which are particularly well matched to the form (2.21): it only

possesses *one* series of monopole modes and *one* (five-fold degenerate) series of quadrupole modes —see next section and Appendix B for details. The existence of so *few* modes which couple to GWs means that *all the absorbed incoming radiation energy will be distributed amongst those few modes only*, thereby making the sphere the *most efficient* detector, even from the sensitivity point of view. The higher energy cross section *per unit mass* reported for spheres on the basis of GR [10], for example, finds here its qualitative explanation. The generality of (2.21), on the other hand, means that *this excellence of the spherical detector is there independently of which is the correct GW theory*.

Before going further, let me mention another potentially useful application of the formalism so far. Cylindrical antennas, for instance, are usually studied in the *thin rod* approximation; although this is generally quite satisfactory, equation (2.21) offers the possibility of eventually considering corrections to such simplifying hypothesis by use of more realistic eigenfunctions, such as those given in [17,18]. Recent new proposals for stumpy cylinder arrays [19] may well benefit from the above approach, too.

### III. THE SPHERICAL ANTENNA

To explore the consequences of (2.21) in a particular case, the mode amplitudes  $\mathbf{u}_N(\mathbf{x})$  and frequencies  $\omega_N$  must be specified. From now on I will focus on a *homogeneous sphere* whose surface is free of tractions and/or tensions; the latter happens to be quite a good approximation, even if the sphere is suspended in the static gravitational field [20].

The normal modes of the free sphere fall into two families: so called *toroidal* —where the sphere only undergoes twistings which keep its shape unchanged throughout the volume— and *spheroidal* [21], where radial as well as tangential displacements take place. I use the notation

$$\mathbf{u}_{nlm}^T(\mathbf{x}) e^{\pm i\omega_{nl}^T t} \quad , \quad \mathbf{u}_{nlm}^P(\mathbf{x}) e^{\pm i\omega_{nl}^P t} \quad (3.1)$$

for them, respectively; note that the index  $N$  of the previous section is a *multiple* index  $\{nlm\}$  for *each* family;  $l$  and  $m$  are the usual *multipole* indices, and  $n$  numbers from 1 to  $\infty$  each of the  $l$ -pole modes. The frequencies happen to be independent of  $m$ , and so every one mode (3.1) is  $(2l+1)$ -fold degenerate. Further details about these eigenmodes are given in Appendix B.

In order to see what (2.21) looks like in this case, integrals of the form (2.6) ought to be evaluated. It is straightforward to prove that they all vanish for the toroidal modes, the spheroidal modes contributing the only non-vanishing terms; after some algebra one finds

$$f_{nlm}^{(S)} \equiv \frac{1}{M} \int_{\text{Sphere}} \mathbf{u}_{nlm}^{P*}(\mathbf{x}) \cdot \mathbf{f}^{(S)}(\mathbf{x}) d^3x = a_n \delta_{l0} \delta_{m0} \quad (3.2a)$$

$$f_{nlm}^{(m')} \equiv \frac{1}{M} \int_{\text{Sphere}} \mathbf{u}_{nlm}^{P*}(\mathbf{x}) \cdot \mathbf{f}^{(m')}(\mathbf{x}) d^3x = b_n \delta_{l2} \delta_{m'm} \quad (3.2b)$$

where

$$a_n = -\frac{1}{M} \int_0^R A_{n0}(r) \rho r^3 dr \quad (3.3a)$$

$$b_n = -\frac{1}{M} \int_0^R [A_{n2}(r) + 3B_{n2}(r)] \rho r^3 dr \quad (3.3b)$$

The functions  $A_{nl}(r)$ ,  $B_{nl}(r)$  are given in Appendix B, and  $R$  is the sphere's radius. To our reassurance, only the monopole and quadrupole *sphere modes* survive, as seen by the presence of the factors  $\delta_{l0}$  and  $\delta_{l2}$  in (3.2a) and (3.2b), respectively. The final series is thus a relatively simple one, even in spite of its generality<sup>2</sup>:

$$\mathbf{u}(\mathbf{x}, t) = \sum_{n=1}^{\infty} \frac{a_n}{\omega_{n0}} \mathbf{u}_{n00}(\mathbf{x}) g_{n0}^{(S)}(t) + \sum_{n=1}^{\infty} \frac{b_n}{\omega_{n2}} \left[ \sum_{m=-2}^2 \mathbf{u}_{n2m}(\mathbf{x}) g_{n2}^{(m)}(t) \right], \quad (t > 0) \quad (3.4)$$

---

<sup>2</sup> From now on I will drop the label  $P$ , meaning *spheroidal* mode, to ease the notation since *toroidal* modes no longer appear in the formulae.

where, it is recalled,

$$g_{nl}^{(S,m)}(t) = \int_0^t g^{(S,m)}(t') \sin \omega_{nl}(t-t') dt', \quad (m = -2, \dots, 2) \quad (3.5)$$

Equation (3.4) constitutes the sphere's response to an arbitrary tidal GW perturbation, and will be used to analyse the sensitivity of the spherical detector in the next section. Before doing so, however, a few comments on the antenna's signal *deconvolution capabilities*, within the context of a completely general metric theory of GWs, are in order.

### A. The deconvolution problem

Let us first of all take the Fourier transform of (3.4):

$$\mathbf{U}(\mathbf{x}, \omega) \equiv \int_{-\infty}^{\infty} \mathbf{u}(\mathbf{x}, t) e^{-i\omega t} dt \quad (3.6)$$

This is seen to be

$$\begin{aligned} \mathbf{U}(\mathbf{x}, \omega) = & \frac{\pi}{i} \sum_{n=1}^{\infty} \frac{a_n}{\omega_{n0}} \mathbf{u}_{n00}(\mathbf{x}) G^{(S)}(\omega) [\delta(\omega - \omega_{n0}) - \delta(\omega + \omega_{n0})] + \\ & + \frac{\pi}{i} \sum_{n=1}^{\infty} \frac{b_n}{\omega_{n2}} \left[ \sum_{m=-2}^2 \mathbf{u}_{n2m}(\mathbf{x}) G^{(m)}(\omega) \right] [\delta(\omega - \omega_{n2}) - \delta(\omega + \omega_{n2})] \end{aligned} \quad (3.7)$$

where  $G^{(S)}(\omega)$  and  $G^{(m)}(\omega)$  are the Fourier transforms of  $g^{(S)}(t)$  and  $g^{(m)}(t)$ , respectively:

$$G^{(S,m)}(\omega) \equiv \int_0^{\infty} g^{(S,m)}(t) e^{-i\omega t} dt \quad (3.8)$$

The  $\delta$ -function factors are of course idealisations corresponding to infinitely long integration times and infinitely narrow resonance linewidths — but the essentials of the ensuing discussion will not be affected by those idealisations.

If the measuring system were (ideally) sensitive to all frequencies, filters could be applied to examine the antenna's oscillations at each monopole and quadrupole frequency: a single transducer would suffice to reveal  $G^{(S)}(\omega)$  around the monopole frequencies  $\omega_{n0}$ , whilst *five* (placed at suitable positions) would be required to calculate the five degenerate amplitudes  $G^{(m)}(\omega)$  around the quadrupole frequencies  $\omega_{n2}$ . Once the *six* functions  $G^{(S,m)}(\omega)$  would have thus been determined, inverse Fourier transforms would give us the functions  $g^{(S,m)}(t)$ , and thereby the six Riemann tensor components  $R_{0i0j}(t)$  through inversion of the second equations (2.20), i.e., as an expansion like (2.15) — only with  $g$ 's instead of  $\mathcal{S}$ 's. Deconvolution would then be complete.

Well, not quite... Knowledge of the Riemann tensor in the *laboratory* frame coordinates is not really sufficient to say the waveform has been completely deconvolved, unless we *also* know the *source position* in the sky. There clearly are two possibilities:

- i) The source position *is* known ahead of time by some other astronomical observation methods. Let me rush to emphasise that, far from trivial or uninteresting, this is a *very important* case to consider, specially during the first stages of GW Astronomy, when any reported GW event will have to be thoroughly checked by all possible means.

If the incidence direction is known, then a rotation must be applied to the just obtained quantities  $R_{0i0j}(t)$ , which takes the laboratory  $z$ -axis into coincidence with the incoming wave propagation vector. A classification procedure must thereafter be applied to the so transformed Riemann tensor in order to see which is the theory (or class of theories) compatible with the actual observations. Such classification procedure has been described in detail in [22].

The spherical antenna is thus seen to have the *capability of furnishing the analyst sufficient information to discern amongst different competing theories of GW physics, whenever the wave incidence direction is known prior to detection.*

- ii) The source position is *not* known at detection time. This makes things more complex, since the above rotation between the laboratory and GW frames cannot be performed.

In order to deconvolve the incidence direction in this case, a specific theory of the GWs *must* be assumed —a given choice being made on the basis of whatever prior information is available or, simply, dictated by the decision to probe a particular theory. Wagoner and Paik [7] propose a method which is useful both for GR and BD theory, their idea being simple and elegant at the same time: since neither of these theories predicts the excitation of the  $m=\pm 1$  quadrupole modes *of the wave*, the source position is determined precisely by the rotation angles which, when applied to the laboratory axes, cause the amplitudes of those *antenna* modes to vanish; the rotated frame is thereby associated to the GW natural frame.

A generalisation of this idea can conceivably be found on the basis of a detailed —and possibly rather casuistic— analysis of the canonical forms of the Riemann tensor for a list of theories of gravity, along the following line of argument: any one particular theory will be characterised by certain (homogeneous) canonical relationships amongst the monopole and quadrupole components of the Riemann tensor,  $g^{(S,m)}(t)$ , and so enforcement of those relations upon rotation of the laboratory frame axes should enable determination of the rotation angles or, equivalently, of the incoming radiation incidence direction. Scalar-tensor theories e.g. have  $g^{(\pm 1)}(t) = 0$  in their canonical forms, hence Wagoner and Paik’s proposal for this particular case.

Before any deconvolution procedure is triggered off, however, it is very important to make sure that it will be *viable*. More precisely, since the transformation from the laboratory to the ultimate canonical frame is going to be linear, *invariants* must be preserved. This means that, even if the source position is unknown, certain theories will forthrightly be *vetoed* by the observed  $R_{0i0j}(t)$  if their predicted invariants are incompatible with the observed ones. To give but an easy example, if  $R_{0i0j}(t)$  is *observed* to have a non-null trace  $R_{0i0i}(t)$ , then a veto on GR will be readily served, and therefore no algorithm based on that theory should be applied.

I would like to make a final remark here. Assume a direction deconvolution procedure has been successfully carried through to the end on the basis of certain GW theory, so that the analyst comes up with a pair of numbers  $(\theta, \varphi)$  expressing the source’s coordinates in the sky. Of course, these numbers will represent the *actual* source position *only if the assumed theory is correct*. Now, how do we know it *is* correct? Strictly speaking, “correctness” of a scientific theory is an *asymptotic* concept —in the sense that the possibility always remains open that new facts be eventually discovered which contradict the theory—, and so *reliability* of the estimate  $(\theta, \varphi)$  of the source position can only be assessed in practice in terms of the *consistency* between the assumed theory and whatever experimental evidence is available *to date*, including, indeed, GW measurements themselves. It is thus very important to have a method to verify that the estimate  $(\theta, \varphi)$  does not contradict the theory which enabled its very determination.

Such verification is a *logical* absurdity if only *one* measurement of position is available; this happens for instance if the recorded signal is a *short burst* of radiation, and so *two antennas* are at least necessary to check consistency in that case. The test would proceed as a check that the time delay between reception of the signal at both detectors is consistent with the calculated  $(\theta, \varphi)^3$ , given their relative position and the wave propagation speed predicted by the assumed theory. If, on the other hand, the signal being tracked is a *long duration* signal, then a single antenna may be sufficient to perform the test by looking at the observed Doppler patterns and checking them against those expected with the given  $(\theta, \varphi)$ .

The above considerations have been made ignoring noise in the detector and monitor systems. A fundamental constraint introduced by noise is that it makes the antenna *bandwidth limited* in sensitivity. As a consequence, any deconvolution procedure is deemed to be incomplete or, rather, *ambiguous* [23], since information about the signal can possibly be retrieved only within a reduced bandwidth, whilst the rest will be lost. I thus come to a detailed discussion of the sensitivity of the spherical GW antenna in the next section.

#### IV. THE SENSITIVITY PARAMETERS

I will consider successively *amplitude* and *energy* sensitivities; the first leads to the concept of *transfer function*, while the second to that of absorption *cross section*. I devote separate subsections to analyse each of them in some detail.

---

<sup>3</sup> Note that the two detectors will agree on the same  $(\theta, \varphi)$ , even if the assumed theory is wrong, since the sphere deformations will be the same if caused by the same signal.

## A. The transfer function

A widely used and useful concept in linear system theory is that of *transfer function* [24]. It is defined as the Fourier transform of the system's impulse response, or as the system's impedance/admittance, and can be inferred from the frequency response function (3.7).

We recall from the previous section that the sphere is a multimode device —due to its monopole and five-fold degenerate quadrupole modes. It appears expedient to define a *multimode* or *vector transfer function* as a useful construct which encompasses all six different modes into a single conceptual block, according to

$$\mathbf{U}(\mathbf{x}, \omega) = \sum_{\alpha} \mathbf{Z}^{(\alpha)}(\mathbf{x}, \omega) G^{(\alpha)}(\omega) \quad (4.1)$$

where  $G^{(\alpha)}(\omega)$  are the six driving terms  $G^{(S,m)}(\omega)$  given in (3.8). The transfer function is  $\mathbf{Z}^{(\alpha)}(\mathbf{x}, \omega)$ , and its “vector” character alluded above is reflected by the *multimode index*  $\alpha$ . Looking at (3.7) it is readily seen that

$$\mathbf{Z}^{(S)}(\mathbf{x}, \omega) = \frac{\pi}{i} \sum_{n=1}^{\infty} \frac{a_n}{\omega_{n0}} \mathbf{u}_{n00}(\mathbf{x}) [\delta(\omega - \omega_{n0}) - \delta(\omega + \omega_{n0})] \quad (4.2a)$$

$$\mathbf{Z}^{(m)}(\mathbf{x}, \omega) = \frac{\pi}{i} \sum_{n=1}^{\infty} \frac{b_n}{\omega_{n2}} \mathbf{u}_{n2m}(\mathbf{x}) [\delta(\omega - \omega_{n2}) - \delta(\omega + \omega_{n2})] \quad (m = -2, \dots, 2) \quad (4.2b)$$

As we observe in these formulae, the sphere's sensitivity to monopole excitations is governed by  $a_n/\omega_{n0}$ , and to quadrupole ones by  $b_n/\omega_{n2}$ . Closed expressions happen to exist for  $a_n$  and  $b_n$ ; using the notation of Appendix B, they are

$$\frac{a_n}{R} = \frac{3 C(n, 0)}{8\pi} \frac{j_2(q_{n0}R)}{q_{n0}R} \quad (4.3a)$$

$$\frac{b_n}{R} = -\frac{3 C(n, 2)}{8\pi} \left[ \beta_3(k_{n2}R) \frac{j_2(q_{n2}R)}{q_{n2}R} - 3 \frac{q_{n2}}{k_{n2}} \beta_1(q_{n2}R) \frac{j_2(k_{n2}R)}{k_{n2}R} \right] \quad (4.3b)$$

Numerical investigation of the behaviour of these coefficients shows that they decay asymptotically as  $n^{-2}$ :

$$a_n, b_n \xrightarrow{n \rightarrow \infty} \text{const} \times n^{-2} \quad (4.4)$$

Likewise, it is found that the frequencies  $\omega_{n0}$  and  $\omega_{n2}$  diverge like  $n$  for large  $n$ , so that  $\mathbf{Z}^{(\alpha)}(\mathbf{x}, \omega)$  drops as  $\omega^{-3}$  for large  $\omega$ . Figures 6 and 7 display a symbolic plot of  $\omega^3 \mathbf{Z}^{(S)}(\mathbf{x}, \omega)$  and  $\omega^3 \mathbf{Z}^{(m)}(\mathbf{x}, \omega)$ , respectively, which illustrates the situation: monopole modes soon reach the asymptotic regime, while there appear to be 3 subfamilies of quadrupole modes regularly intertwined; the asymptotic regime for these subfamilies is more irregularly reached. Note also the perfectly regular alternate changes of phase (by  $\pi$  radians) in both monopole and each quadrupole family.

The sharp fall in sensitivity of a sphere for higher frequency modes ( $n^{-3}$ ) indicates that only the lowest ones stand a chance of being observable in an actual GW antenna. I report in Table I the numerical values of the relevant parameters for the first few monopole and quadrupole modes. The reason for the last (fourth) columns will become clear later.

## B. The absorption cross section

Let us calculate now the energy of the oscillating sphere. We first define the *spectral energy density* at frequency  $\omega$ , which is naturally given by<sup>4</sup>

$$W(\omega) = \frac{1}{T} \int_{\text{Solid}} \frac{1}{2} \omega^2 |\mathbf{U}(\mathbf{x}, \omega)|^2 \rho d^3x \quad (4.5)$$

---

<sup>4</sup>  $T$  is the integration time —assumed very large. The peaks in the  $\delta$ -functions diverge like  $T/\pi$ .



TABLE I. First few monopole (left) and quadrupole (right) sphere parameters, for a  $\sigma=0.33$  material. First and second columns on either side of the central line number the modes and give the corresponding eigenvalue; rows are intertwined in order of ascending frequency, which is proportional to  $kR$  —see (B6) below. Third columns contain the  $a_n$  and  $b_n$  coefficients defined in equations (3.3a) and (3.3b), respectively; the fourth columns display the cross section *ratios*  $(k_{10}a_1/k_{n0}a_n)^2$  and  $(k_{12}b_1/k_{n2}b_n)^2$  for higher frequency modes, respectively, taking as reference the lowest in each family —cf. equations (4.18).

$n$	$k_{n0}R$	$a_n/R$	$\sigma_{10}/\sigma_{n0}$	$n$	$k_{n2}R$	$b_n/R$	$\sigma_{12}/\sigma_{n2}$
				1	2.650	0.328	1
				2	5.088	0.106	2.61
1	5.432	0.214	1	3	8.617	$-1.907 \times 10^{-2}$	27.95
				4	10.917	$-9.101 \times 10^{-3}$	76.42
2	12.138	$-3.772 \times 10^{-2}$	6.46	5	12.280	$1.387 \times 10^{-2}$	25.99
				6	15.347	$6.879 \times 10^{-3}$	67.87
3	18.492	$1.600 \times 10^{-2}$	15.49				

and can be easily evaluated:

$$\begin{aligned}
W(\omega) = & \frac{1}{2}\pi M \sum_{n=1}^{\infty} a_n^2 \left| G^{(S)}(\omega) \right|^2 [\delta(\omega - \omega_{n0}) + \delta(\omega + \omega_{n0})] + \\
& + \frac{1}{2}\pi M \sum_{n=1}^{\infty} b_n^2 \left[ \sum_{m=-2}^2 \left| G^{(m)}(\omega) \right|^2 \right] [\delta(\omega - \omega_{n2}) + \delta(\omega + \omega_{n2})]
\end{aligned} \tag{4.6}$$

The *energy* at any one spectral frequency  $\omega_{nl}$  is obtained by *integration* of the spectral density in a narrow interval around  $\omega = \pm\omega_{nl}$ :

$$E(\omega_{nl}) = \int_{-\omega_{nl}-\varepsilon}^{-\omega_{nl}+\varepsilon} + \int_{\omega_{nl}-\varepsilon}^{\omega_{nl}+\varepsilon} W(\omega) \frac{d\omega}{2\pi} \tag{4.7}$$

In particular,

$$E(\omega_{n0}) = \frac{1}{2} M a_n^2 \left| G^{(S)}(\omega_{n0}) \right|^2 \tag{4.8a}$$

$$E(\omega_{n2}) = \frac{1}{2} M b_n^2 \sum_{m=-2}^2 \left| G^{(m)}(\omega_{n2}) \right|^2 \tag{4.8b}$$

The sensitivity parameter associated with the vibrational energy of the modes is the detector's *absorption cross section*, defined as the energy it absorbs per unit incident GW spectral flux density, or

$$\sigma_{\text{abs}}(\omega) = \frac{E(\omega)}{\Phi(\omega)} \tag{4.9}$$

where  $\Phi(\omega)$  is the number of joules per square metre and Hz carried by the GW at frequency  $\omega$  as it passes by the antenna. Thus, for the frequencies of interest,

$$\sigma_{\text{abs}}(\omega_{n0}) = \frac{1}{2} M a_n^2 \frac{\left| G^{(S)}(\omega_{n0}) \right|^2}{\Phi(\omega_{n0})} \tag{4.10a}$$

$$\sigma_{\text{abs}}(\omega_{n2}) = \frac{1}{2} M b_n^2 \frac{\sum_{m=-2}^2 \left| G^{(m)}(\omega_{n2}) \right|^2}{\Phi(\omega_{n2})} \tag{4.10b}$$

These quantities have very precise values, but such values can only be calculated on the basis of a *specific underlying theory of the GW physics*. In the absence of such theory, neither  $\Phi(\omega)$  nor  $G^{(S,m)}(\omega)$  can possibly be calculated, since

they are *not* theory independent quantities. To date, only GR calculations have been reported in the literature [7,9,10]. As I will now show, even though the fractions in the rhs of (4.10) are *not* theory independent, some very general results can still be obtained about the sphere’s cross section within the context of metric theories of the gravitational interaction. To do so, it will be necessary to go into a short digression on the general nature of weak metric GWs.

No matter which is the (metric) theory which happens to be the “correct one” to describe gravitation, it is beyond reasonable doubt that any GWs reaching the Earth ought to be *very weak*. The linear approximation should therefore be an extremely good one to describe the propagating field variables in the neighbourhood of the detector. In such circumstances, the field equations can be derived from a Poincaré invariant variational principle based on an action integral of the type

$$\int \mathcal{L}(\psi_A, \psi_{A,\mu}) d^4x \quad (4.11)$$

where the Lagrangian density  $\mathcal{L}$  is a *quadratic* functional of the field variables  $\psi_A(x)$  and their space-time derivatives  $\psi_{A,\mu}(x)$ ; these variables include the metric perturbations  $h_{\mu\nu}$ , plus any other fields required by the specific theory under consideration —e.g. a scalar field in the theory of Brans–Dicke, etc. The requirement that  $\mathcal{L}$  be quadratic ensures that the Euler–Lagrange equations of motion are *linear*.

The energy and momentum transported by the waves can be calculated in this formalism in terms of the components  $\tau^{\mu\nu}$  of the canonical energy-momentum tensor<sup>5</sup>

$$\tau^{\mu\nu}(\mathbf{x}, t) = \sum_A \frac{\partial \mathcal{L}}{\partial \psi_{A,\mu}} \psi_A^{\prime\nu} - \mathcal{L} \eta^{\mu\nu} \quad (4.12)$$

The flux energy density, or Poynting, vector is given by  $S_i = c^2 \tau^{0i}$ , i.e.,

$$\mathbf{S}(\mathbf{x}, t) = c^3 \sum_A \frac{\partial \mathcal{L}}{\partial \dot{\psi}_A} \nabla \psi_A \quad (4.13)$$

where  $\dot{\phantom{x}} \equiv \partial/\partial t$ . Any GW hitting the antenna will be seen plane, due to the enormous distance to the source. If  $\mathbf{k}$  is the incidence direction (normal to the wave front), then the fields will depend on the variable  $ct - \mathbf{k} \cdot \mathbf{x}$ , so that the GW energy reaching the detector per unit time and area is

$$\phi(t) \equiv \mathbf{k} \cdot \mathbf{S}(\mathbf{x}, t) = -c^2 \sum_A \frac{\partial \mathcal{L}}{\partial \dot{\psi}_A} \dot{\psi}_A \quad (4.14)$$

where  $\mathbf{x}$  is the sphere’s centre position relative to the source —which is *fixed*, and so its dependence can be safely dropped in the lhs of the above expression. The important thing to note in equation (4.14) is that it tells us that  $\phi(t)$  *can be written as a quadratic form in the time derivatives of the fields*  $\psi_A$ . As a consequence, the spectral density  $\Phi(\omega)$ , defined by

$$\int_{-\infty}^{\infty} \phi(t) dt = \int_0^{\infty} \Phi(\omega) \frac{d\omega}{2\pi} \quad (4.15)$$

can be ascertained to factorise as

$$\Phi(\omega) = \omega^2 \Phi_0(\omega) \quad (4.16)$$

where  $\Phi_0(\omega)$  is again a *quadratic* function of the Fourier transforms  $\Psi_A(\omega)$  of the fields  $\psi_A$ . On the other hand, the functions  $G^{(S,m)}(\omega)$  in (4.10) which, it is recalled, are the Fourier transforms of  $g^{(S,m)}(t)$  in (2.20), contain *second* order derivatives of the *metric* fields  $h_{\mu\nu}$ , and therefore of *all* the fields  $\psi_A$  as a result of the theory’s field equations. Since we are considering *plane wave* solutions to those equations, all derivatives can be reduced to *time* derivatives —just like in (4.14) above. We can thus write

---

<sup>5</sup> This tensor is *not* symmetric in general, but can be symmetrized by a standard method due to Belinfante [25,26]. For the considerations which follow in this paper it is unnecessary to go into those details, and the *canonical* form (4.12) will be sufficient.

$$G^{(S,m)}(\omega) = -\omega^2 \Psi^{(S,m)}(\omega) \quad (4.17)$$

with  $\Psi^{(S,m)}(\omega)$  suitable *linear* combinations of the  $\Psi_A(\omega)$ . Replacing the last two equations into (4.10) and manipulating dimensions expediently, we come to the remarkable result that

$$\sigma_{\text{abs}}(\omega_{n0}) = K_S(\aleph) \frac{GMv_t^2}{c^3} (k_{n0}a_n)^2 \quad (4.18a)$$

$$\sigma_{\text{abs}}(\omega_{n2}) = K_Q(\aleph) \frac{GMv_t^2}{c^3} (k_{n2}b_n)^2 \quad (4.18b)$$

where  $v_t^2 \equiv (2+2\sigma)^{-1} v_s^2$ ,  $v_s$  being the speed of sound in the detector's material, and  $\sigma$  its Poisson ratio;  $G$  is the Gravitational constant. The “remarkable” about the above is that the coefficients  $K_S(\aleph)$  and  $K_Q(\aleph)$  are *independent of frequency*: they *exclusively depend on the underlying gravitation theory*, which I symbolically denote by  $\aleph$ . To see that this is the case, it is enough to consider a monochromatic incident wave: since the coefficients  $K_S(\aleph)$  and  $K_Q(\aleph)$  happen to be *invariant* with respect to field amplitude *scalings*, this means they will *only* depend on the amplitudes' relative weights, i.e., on the field equations' *specific structure*.

By way of example, it is interesting to see what the results for General Relativity (GR) and Brans–Dicke (BD) theory are. After somehow lengthy algebra it is found that

$$\aleph = \text{GR} \Rightarrow \begin{cases} K_S(\aleph) = 0 \\ K_Q(\aleph) = \frac{16\pi^2}{15} \end{cases} \quad (4.19)$$

and

$$\aleph = \text{BD} \Rightarrow \begin{cases} K_S(\aleph) = \frac{8\pi^2}{9} (3+2\Omega)^{-2} k \left[ 1 + \frac{k\Omega}{(3+2\Omega)^2} \right]^{-1} \\ K_Q(\aleph) = \frac{16\pi^2}{15} \left[ 1 + \frac{1}{6} (3+2\Omega)^{-2} k \right] \left[ 1 + \frac{k\Omega}{(3+2\Omega)^2} \right]^{-1} \end{cases} \quad (4.20)$$

In the latter formulae,  $\Omega$  is the usual Brans–Dicke parameter  $\omega$  [27], renamed here to avoid confusion with *frequency*, and  $k$  is a dimensionless parameter, generally of order one, depending on the source's properties [28]. As is well known, GR is obtained in the limit  $\Omega \rightarrow \infty$  of BD [15]; the quoted results are of course in agreement with that limit.

Incidentally, an interesting consequence of the above equations is this: though not explicitly shown in this paper (see, however, reference [7]), the presence of a scalar field in the theory of Brans and Dicke causes *not only the monopole* sphere's modes to be excited, *but also the  $m=0$  quadrupole ones*; what we see in equations (4.20) is that *precisely* 5/6 of the total energy extracted from the scalar wave goes into the antenna's monopole modes, whilst there is still a remaining 1/6 which is communicated to the quadrupoles, independently of the values of  $\Omega$  and  $k$ <sup>6</sup>. This somehow non-intuitive result finds its explanation in the structure of the Riemann tensor in BD theory, in which the *excess*  $R_{0i0j}$  with respect to General Relativity happens *not* to be proportional to the scalar part  $E_{ij}^{(S)}$ , but to a combination of  $E_{ij}^{(S)}$  and  $E_{ij}^{(0)}$ .

Equations (4.18) show that, no matter which is the gravity theory assumed, the sphere's absorption cross sections for higher modes *scale* as the successive coefficients  $(k_{n0}a_n)^2$  and  $(k_{n2}b_n)^2$  for monopole and quadrupole modes, respectively. In particular, the result quoted in [10] that cross section for the second quadrupole mode is 2.61 times less than that for the first, assuming GR, is in fact valid, as we now see, *independently of which is the (metric) theory of gravity actually governing GW physics*. The fourth columns in Table I display these scaling properties. It is seen that the drop in cross section from the first to the second monopole mode is as high as 6.46. It should however be stressed that the frequency of such mode would be over 4 kHz for a (likely) sphere whose fundamental *quadrupole* frequency be 900 Hz [10]. Note finally the asymptotic cross section drop as  $n^{-2}$  for large  $n$  —cf. equation (4.4) and the ensuing paragraph.

---

<sup>6</sup> Note however that since monopole and quadrupole detector modes occur at different frequencies, this particular *distribution* of energy may not be seen if the sphere's vibrations are monitored at a single resonance.

## V. CONCLUSION

The main purpose of this paper has been to set up a *sound* mathematical formalism to tackle with as much generality as possible any questions related to the interaction between a resonant antenna and a weak incoming GW, with much special emphasis on the homogeneous *sphere*. New results have been found along this line, such as the *scaling* properties of cross sections for higher frequency modes, or the sensitivity of the antenna to arbitrary metric GWs; also, new ideas have been put forward regarding the *direction deconvolution* problem within the context of an arbitrary metric theory of GW physics. Less spectacularly, the full machinery has also been applied to produce *independent* checks of previously published results.

The whole investigation reported herein has been developed with no *a priori* assumptions about any specific (metric) theory of the GWs, and is therefore *very* general. “Too general solutions” are often impractical in science; here, however, the “very general” appears to be rather “cheap”, as seen in the results expressed by the equations of section 3 above. An immediate consequence is that solid elastic detectors of GWs (and, in particular, spheres) offer, as a matter of principle, the possibility of probing *any* given theory of GW physics with just as much effort as it would take, e.g., to probe General Relativity: the vector transfer function of section 4 supplies the requisite theoretical vehicle for the purpose.

An important question, however, has not been considered in this paper. This is the *transducer* problem: the sphere’s oscillations can only be revealed to the observer by means of suitable (usually electromechanical) transducers. These devices, however, are not *neutral*, i.e., they *couple* to the antenna’s motions, thereby exercising a back action on it which must be taken into consideration if one is to correctly interpret the system’s readout. Preliminary studies and proposals have already been published [8], but further work is clearly needed for a more thorough understanding of the problems involved.

Progress in this direction is currently being made —which I expect to report on shortly. The formalism developed in this paper provides basic support to that further work.

## ACKNOWLEDGMENTS

It is a pleasure for me to thank Eugenio Coccia for his critical reading and comments on the manuscript, and to JMM Senovilla for having devoted a part of his time to enlightening discussions with me on the geometrical nature and properties of metric GWs. I also want to express gratitude to M Montero and JA Ortega for their assistance during the first stages of this work. I have received support from the Spanish Ministry of Education through contract number PB93–1050.

## APPENDIX A:

Let  $\mathbf{e}_x, \mathbf{e}_y, \mathbf{e}_z$  be three orthonormal Cartesian vectors defining the sphere’s laboratory reference frame. We define the equivalent triad

$$\mathbf{e}^{(0)} = \mathbf{e}_z \quad , \quad \mathbf{e}^{(\pm 1)} = \frac{1}{\sqrt{2}} (\mathbf{e}_x \pm i\mathbf{e}_y) \quad (\text{A1})$$

having the properties

$$\mathbf{e}^{*(m')} \cdot \mathbf{e}^{(m)} = \delta_{m'm} \quad , \quad m, m' = -1, 0, 1 \quad (\text{A2})$$

We say that the vectors (A1) are the *natural basis* for the  $l=1$  irreducible representation of the rotation group; they behave under arbitrary rotations precisely like the spherical harmonics  $Y_{1m}(\theta, \varphi)$ . In particular, if a rotation of angle  $\alpha$  around the  $z$ -axis is applied to the original frame, then

$$\mathbf{e}^{(\pm 1)} \rightarrow \exp(\pm i\alpha) \mathbf{e}^{(\pm 1)} \quad , \quad \mathbf{e}^{(0)} \rightarrow \mathbf{e}^{(0)} \quad (\text{A3})$$

Higher rank tensors have specific multipole characteristics depending on the number of tensor indices, and the above basis lends itself to reveal those characteristics, too. For example, the five dimensional linear space of traceless symmetric tensors supports the  $l=2$  irreducible representation of the rotation group, while a tensor’s trace is an invariant. A general symmetric tensor can be expressed as an “orthogonal” sum of a traceless symmetric tensor and a multiple of the unit tensor. A convenient basis to expand any such tensor is the following:

$$\mathbf{e}^{(1)} \otimes \mathbf{e}^{(1)} \quad , \quad \mathbf{e}^{(-1)} \otimes \mathbf{e}^{(-1)} \quad (A4a)$$

$$\mathbf{e}^{(0)} \otimes \mathbf{e}^{(1)} + \mathbf{e}^{(1)} \otimes \mathbf{e}^{(0)} \quad , \quad \mathbf{e}^{(0)} \otimes \mathbf{e}^{(-1)} + \mathbf{e}^{(-1)} \otimes \mathbf{e}^{(0)} \quad (A4b)$$

$$\mathbf{e}^{(1)} \otimes \mathbf{e}^{(-1)} + \mathbf{e}^{(-1)} \otimes \mathbf{e}^{(1)} - 2 \mathbf{e}^{(0)} \otimes \mathbf{e}^{(0)} \quad (A4c)$$

$$\mathbf{e}^{(1)} \otimes \mathbf{e}^{(-1)} + \mathbf{e}^{(-1)} \otimes \mathbf{e}^{(1)} + \mathbf{e}^{(0)} \otimes \mathbf{e}^{(0)} \quad (A4d)$$

The elements (A4a) get multiplied by  $e^{\pm 2i\alpha}$  in a rotation of angle  $\alpha$  around the  $z$ -axis, respectively, the (A4b) by  $e^{\pm i\alpha}$ , and (A4c) and (A4d) are invariant, as is readily seen. These properties define the “spin characteristics” of the corresponding tensors. Also, the five elements (A4a)–(A4c) are *traceless* tensors, while (A4d) is the *unit* tensor. Any symmetric tensor can be expressed as a linear combination of the six (A4), and the respective coefficients carry the information about the weights of the different monopole and quadrupole components of the tensor.

Equations (2.16) in the text are the matrix representation of the above tensors in the Cartesian basis  $\mathbf{e}_x, \mathbf{e}_y, \mathbf{e}_z$ , except that they are multiplied by suitable coefficients to ensure that the conditions

$$E_{ij}^{(S)} n_i n_j = Y_{00}(\theta, \varphi) \quad , \quad E_{ij}^{(m)} n_i n_j = Y_{2m}(\theta, \varphi) \quad (A5)$$

where  $\mathbf{n} \equiv \mathbf{x}/|\mathbf{x}|$  is the radial unit vector, hold. They are arbitrary, but expedient for the calculations in this paper. The following *orthogonality* relations can be easily established:

$$E_{ij}^{*(m')} E_{ij}^{(m)} = \frac{15}{8\pi} \delta_{m'm} \quad , \quad E_{ij}^{(S)} E_{ij}^{(m)} = 0 \quad , \quad E_{ij}^{(S)} E_{ij}^{(S)} = \frac{3}{4\pi} \quad (A6)$$

with the indices  $m, m'$  running from  $-2$  to  $2$ , and with an understood sum over the repeated  $i$  and  $j$ . It is also easy to prove the *closure* properties

$$E_{ij}^{(S)} E_{kl}^{(S)} + \frac{2}{5} \sum_{m=-2}^2 E_{ij}^{*(m)} E_{kl}^{(m)} = \frac{3}{8\pi} (\delta_{ik} \delta_{jl} + \delta_{il} \delta_{jk}) \quad (A7)$$

Equations (A6) and (A7) constitute the *completeness* equations of the  $E$ -matrix basis of Euclidean symmetric tensors.

## APPENDIX B:

This Appendix is intended to give a rather complete summary of the frequency spectrum and eigenmodes of a uniform elastic sphere. Although this is a classical problem in Elasticity Theory [29], some of the results which follow have never been published so far. Also, its scope is to serve as reference for notation, etc., in future work.

The uniform<sup>7</sup> elastic sphere's normal modes are obtained as the solutions to the eigenvalue equation

$$\mu \nabla^2 \mathbf{u} + (\lambda + \mu) \nabla(\nabla \cdot \mathbf{u}) = -\omega^2 \rho \mathbf{u} \quad (B1)$$

with the boundary conditions that its surface be free of any tensions and/or tractions; this is expressed by the equations [11]

$$\sigma_{ij} n_j = 0 \quad \text{at } r=R \quad (B2)$$

where  $R$  is the sphere's radius,  $\mathbf{n}$  the outward normal, and  $\sigma_{ij}$  the *stress* tensor

$$\sigma_{ij} = \lambda u_{kk} \delta_{ij} + 2\mu u_{ij} \quad (B3)$$

with  $u_{ij} \equiv \frac{1}{2}(u_{i,j} + u_{j,i})$ , the *strain* tensor, and  $\lambda, \mu$  the Lamé coefficients [11].

Like any differentiable vector field,  $\mathbf{u}(\mathbf{x})$  can be expressed as a sum of an irrotational vector and a divergence-free vector,

$$\mathbf{u}(\mathbf{x}) = \mathbf{u}_{\text{irrot.}}(\mathbf{x}) + \mathbf{u}_{\text{div-free}}(\mathbf{x}) \quad , \quad (B4)$$

---

<sup>7</sup> By *uniform* I mean its density  $\rho$  is constant throughout the solid in the unperturbed state.

say; on substituting this into equation (B1), and after a few easy manipulations, one can see that

$$(\nabla^2 + k^2) \mathbf{u}_{\text{div-free}}(\mathbf{x}) = 0, \quad (\nabla^2 + q^2) \mathbf{u}_{\text{irrot.}}(\mathbf{x}) = 0 \quad (\text{B5})$$

where

$$k^2 \equiv \frac{\rho\omega^2}{\mu}, \quad q^2 \equiv \frac{\rho\omega^2}{\lambda + 2\mu} \quad (\text{B6})$$

Now the irrotational component can generically be expressed as the *gradient* of a scalar function, i.e.,

$$\mathbf{u}_{\text{irrot.}}(\mathbf{x}) = \nabla\phi(\mathbf{x}) \quad (\text{B7})$$

while there are *two* linearly independent divergence-free components which, as can be readily verified, are

$$\mathbf{u}_{\text{div-free}}^{(1)}(\mathbf{x}) = \mathbf{L}\psi^{(1)}(\mathbf{x}), \quad \text{and} \quad \mathbf{u}_{\text{div-free}}^{(2)}(\mathbf{x}) = \nabla \times \mathbf{L}\psi^{(2)}(\mathbf{x}) \quad (\text{B8})$$

where  $\mathbf{L} \equiv -i\mathbf{x} \times \nabla$  is the ‘‘angular momentum’’ operator, cf. [16], and  $\psi^{(1)}$  and  $\psi^{(2)}$  are also scalar functions. If (B7) and (B8) are now respectively substituted in (B5), it is found that  $\phi(\mathbf{x})$ ,  $\psi^{(1)}(\mathbf{x})$ , and  $\psi^{(2)}(\mathbf{x})$  satisfy Helmholtz equations:

$$(\nabla^2 + k^2)\psi(\mathbf{x}) = 0, \quad (\nabla^2 + q^2)\phi(\mathbf{x}) = 0 \quad (\text{B9})$$

where  $\psi(\mathbf{x})$  stands for either  $\psi^{(1)}(\mathbf{x})$  or  $\psi^{(2)}(\mathbf{x})$ . Therefore

$$\phi(\mathbf{x}) = j_l(qr) Y_{lm}(\mathbf{n}), \quad \psi(\mathbf{x}) = j_l(kr) Y_{lm}(\mathbf{n}) \quad (\text{B10})$$

in order to ensure regularity at the centre of the sphere,  $r=0$ . Here,  $j_l$  is a *spherical* Bessel function —see [30] for general conventions on these functions—, and  $Y_{lm}$  a spherical harmonic [16]. Finally thus,

$$\mathbf{u}(\mathbf{x}) = \frac{C_0}{q^2} \nabla\phi(\mathbf{x}) + \frac{iC_1}{k} \mathbf{L}\psi(\mathbf{x}) + \frac{iC_2}{k^2} \nabla \times \mathbf{L}\psi(\mathbf{x}) \quad (\text{B11})$$

where  $C_0, C_1, C_2$  are three constants which will be determined by the boundary conditions (B2) (the denominators under them have been included for notational convenience). After lengthy algebra, those conditions can be expressed as the following system of linear equations:

$$\left[ \beta_2(qR) - \frac{\lambda}{2\mu} q^2 R^2 \beta_0(qR) \right] C_0 - l(l+1) \beta_1(kR) C_2 = 0 \quad (\text{B12a})$$

$$\beta_1(kR) C_1 = 0 \quad (\text{B12b})$$

$$\beta_1(qR) C_0 - \left[ \frac{1}{2} \beta_2(kR) + \left\{ \frac{l(l+1)}{2} - 1 \right\} \beta_0(kR) \right] C_2 = 0 \quad (\text{B12c})$$

where

$$\beta_0(z) \equiv \frac{j_l(z)}{z^2}, \quad \beta_1(z) \equiv \frac{d}{dz} \left[ \frac{j_l(z)}{z} \right], \quad \beta_2(z) \equiv \frac{d^2}{dz^2} [j_l(z)] \quad (\text{B13})$$

There are clearly *two* families of solutions to (B12):

i) *Toroidal* modes. These are characterised by

$$\beta_1(kR) = 0, \quad C_0 = C_2 = 0 \quad (\text{B14})$$

The frequencies of these modes are *independent* of  $\lambda$ , and thence independent of the material’s Poisson ratio. Their amplitudes are

$$\mathbf{u}_{nlm}^T(\mathbf{x}) = T_{nl}(r) i\mathbf{L}Y_{lm}(\mathbf{n}) \quad (\text{B15})$$

with

$$T_{nl}(r) = C_1(n, l) j_l(k_{nl}r) \quad (\text{B16})$$

and  $C_1(n, l)$  a dimensionless normalisation constant determined by the general formula (2.8);  $k_{nl}R$  is the  $n$ -th root of the first equation (B14) for a given  $l$ .

ii) *Spheroidal* modes. These correspond to

$$\det \begin{pmatrix} \beta_2(qR) - \frac{\lambda}{2\mu} q^2 R^2 \beta_0(qR) & l(l+1) \beta_1(kR) \\ \beta_1(qR) & \frac{1}{2} \beta_2(kR) + \left\{ \frac{l(l+1)}{2} - 1 \right\} \beta_0(kR) \end{pmatrix} = 0 \quad (\text{B17})$$

and  $C_1 = 0$ . The frequencies of these modes *do* depend on the Poisson ratio, and their amplitudes are

$$\mathbf{u}_{nlm}^P(\mathbf{x}) = A_{nl}(r) Y_{lm}(\mathbf{n}) \mathbf{n} - B_{nl}(r) i\mathbf{n} \times \mathbf{L} Y_{lm}(\mathbf{n}) \quad (\text{B18})$$

where  $A_{nl}(r)$  and  $B_{nl}(r)$  have the somewhat complicated form

$$A_{nl}(r) = C(n, l) \left[ \beta_3(k_{nl}R) j_l'(q_{nl}r) - l(l+1) \frac{q_{nl}}{k_{nl}} \beta_1(q_{nl}R) \frac{j_l(k_{nl}r)}{k_{nl}r} \right] \quad (\text{B19a})$$

$$B_{nl}(r) = C(n, l) \left[ \beta_3(k_{nl}R) \frac{j_l(q_{nl}r)}{q_{nl}r} - \frac{q_{nl}}{k_{nl}} \beta_1(q_{nl}R) \frac{\{k_{nl}r j_l(k_{nl}r)\}'}{k_{nl}r} \right] \quad (\text{B19b})$$

with accents denoting derivatives with respect to implied (dimensionless) arguments,

$$\beta_3(z) \equiv \frac{1}{2} \beta_2(z) + \left\{ \frac{l(l+1)}{2} - 1 \right\} \beta_0(z) \quad (\text{B20})$$

and  $C(n, l)$  a new normalisation constant. It is understood that  $q_{nl}$  and  $k_{nl}$  are obtained after the (transcendental) equation (B17) has been solved for  $\omega$  —cf. equation (B6).

In actual practice equations (B14) and (B17) are solved for the *dimensionless* quantity  $kR$ , which will hereafter be called the *eigenvalue*. In view of (B6), the relationship between the latter and the measurable frequencies (in Hz) is given by

$$\nu \equiv \frac{\omega}{2\pi} = \left( \frac{\mu}{\rho R^2} \right)^{1/2} \frac{kR}{2\pi} \quad (\text{B21})$$

It is more useful to express the frequencies in terms of the Poisson ratio,  $\sigma$ , and of the speed of sound  $v_s$  in the selected material. For this the following formulas are required —see e.g. [11]:

$$v_s = \sqrt{\frac{Y}{\rho}} \quad (\text{B22})$$

where  $Y$  is the *Young modulus*, related to the Lamé coefficients and the Poisson ratio by

$$Y = \frac{(3\lambda + 2\mu)\mu}{\lambda + \mu} = 2(1 + \sigma)\mu, \quad \sigma \equiv \frac{\lambda}{2(\lambda + \mu)} \quad (\text{B23})$$

Hence,

$$\nu = \frac{(kR)}{2\pi \sqrt{1 + \sigma}} \frac{v_s}{R} \quad (\text{B24})$$

Equation (B24) provides a suitable transformation formula from abstract number eigenvalues ( $kR$ ) into physical frequencies  $\nu$ , for given material's properties and sizes.

Tables III and II respectively display a set of values of ( $kR$ ) for *toroidal* and *spheroidal* modes. While GWs can only couple to quadrupole and monopole modes, it is important to have some detailed knowledge of analytical results, as the sphere's frequency spectrum is rather involved. It often happens, both in numerical simulations and in experimental determinations, that it is very difficult to disentangle the wealth of observed frequency lines, and to correctly associate them with the corresponding eigenmode. Complications are further enhanced by partial degeneracy lifting found in practice (due to broken symmetries), which result in even more frequency lines in the spectrum. Accurate analytic results should therefore be very helpful to assist in frequency identification tasks.

TABLE II. List of a few *spheroidal eigenvalues*, ordered in columns of ascending harmonics for each multipole value. Spheroidal eigenvalues depend on the sphere’s material Poisson ratio —although this dependence is weak. In this table, values are given for  $\sigma = 0.33$ . Note that the table contains *all* eigenvalues less than or equal to 11.024 yet is not exhaustive for values larger than that one; this would require to stretch the table horizontally beyond  $l = 10$  —see Figure I for a qualitative inspection of trends in eigenvalue progressions.

$n$	$l = 0$	$l = 1$	$l = 2$	$l = 3$	$l = 4$	$l = 5$	$l = 6$	$l = 7$	$l = 8$	$l = 9$	$l = 10$
1	5.4322	3.5895	2.6497	3.9489	5.0662	6.1118	7.1223	8.1129	9.0909	10.061	11.024
2	12.138	7.2306	5.0878	6.6959	8.2994	9.8529	11.340	12.757	14.111	15.410	16.665
3	18.492	8.4906	8.6168	9.9720	11.324	12.686	14.066	15.462	16.867	18.272	19.664
4	24.785	10.728	10.917	12.900	14.467	15.879	17.243	18.589	19.930	21.272	22.619
5	31.055	13.882	12.280	14.073	16.125	18.159	19.997	21.594	23.043	24.426	25.778

TABLE III. List of a few *toroidal eigenvalues*, ordered in columns of ascending harmonics for each multipole value. Unlike spheroidal eigenvalues, toroidal eigenvalues are independent of the sphere’s material Poisson ratio. Note that the table contains *all* eigenvalues less than or equal to 12.866 yet is not exhaustive for values larger than that one; this would require to stretch the table horizontally beyond  $l = 11$  —see Figure II for a qualitative inspection of trends in eigenvalue progressions.

$n$	$l = 1$	$l = 2$	$l = 3$	$l = 4$	$l = 5$	$l = 6$	$l = 7$	$l = 8$	$l = 9$	$l = 10$	$l = 11$
1	5.7635	2.5011	3.8647	5.0946	6.2658	7.4026	8.599	9.6210	10.711	11.792	12.866
2	9.0950	7.1360	8.4449	9.7125	10.951	12.166	13.365	14.548	15.720	16.882	18.035
3	12.323	10.515	11.882	13.211	14.511	15.788	17.045	18.287	19.515	20.731	21.937
4	15.515	13.772	15.175	16.544	17.886	19.204	20.503	21.786	23.055	24.310	25.555
5	18.689	16.983	18.412	19.809	21.181	22.530	23.860	25.174	26.473	27.760	29.035

In Figures 1 and 2 a symbolic line diagramme of the two families of frequencies of the sphere’s spectrum is presented. Spheroidal eigenvalues have been plotted for the Poisson ratio  $\sigma=0.33$ . Although only the  $l=0$  and  $l=2$  *spheroidal* series couple to GW tidal forces, the plots include other eigenvalues, as they can be useful both in bench experiments —cf. equation (2.12) above— and for vetoing purposes in a spherical antenna.

Figures 3, 4 and 5 contain plots of the first three monopole and quadrupole functions  $T_{nl}(r)$ ,  $A_{nl}(r)$  and  $B_{nl}(r)$ , always for  $\sigma=0.33$ .  $T_{n0}(r)$  and  $B_{n0}(r)$  have however been omitted; this is because they are multiplied by an identically zero angular coefficient in the amplitude formulae (B15) and (B18). Indeed, monopole vibrations are spherically symmetric, i.e., purely radial.

- 
- [1] See e.g. Hamilton O.W. in Gleiser R.J., Kozameh C.N. and Moreschi O.M., *Proceedings of GR13, Córdoba, Argentina*, IOP 1993. Also, Hamilton O.W. in *Proceedings of the First Edoardo Amaldi Meeting* (Frascati 1994), to appear.
  - [2] Astone P. *et al*, *Phys. Rev.* **D47**, 2 (1993).
  - [3] Astone P. *et al.*, *Europhys. Lett.* **16**, 231 (1991).
  - [4] Eugenio Coccia, personal communication.
  - [5] Forward R., *Gen. Rel. and Grav.* **2**, 149 (1971).
  - [6] Ashby N. and Dreitlein J., *Phys. Rev.* **D12**, 336 (1975).
  - [7] Wagoner R. V. and Paik H. J. in *Experimental Gravitation*, Proceedings of the Pavia International Symposium, Acad. Naz. dei Lincei 1977.
  - [8] Johnson W. and Merkowitz S. M., *Phys. Rev. Lett.* **70**, 2367 (1993).
  - [9] Michelson P.F. and Zhou C.Z., submitted to *Phys Rev D* (1994).
  - [10] Coccia E., Lobo J.A. and Ortega J.A., submitted to *Physical Review Letters* (1994).
  - [11] Landau L.D. and Lifshitz E.M., *Theory of Elasticity*, Pergamon 1970.
  - [12] Tym Myint-U, *Partial Differential Equations for Scientists and Engineers*, North Holland 1987.
  - [13] Warren Johnson, private communication during the First Edoardo Amaldi Meeting in Frascati, june 1994.
  - [14] Misner, Thorne, Wheeler, *Gravitation*, Freeman 1973.



- [15] Weinberg S., *Gravitation and Cosmology*, Wiley 1972.
- [16] Edmonds A.R., *Angular Momentum in Quantum Mechanics*, Princeton Univ. Press 1960.
- [17] Rasband S.N., *J Acous Soc Am* **57**, 899 (1975).
- [18] Hier R.G. and Rasband S.N., *Ap Jour* **195**, 507 (1975).
- [19] Bassan M., Cosmelli C., Frasca S., Papa M.A., Puppo P., Rapagnani P. and Ricci F., *High Frequency Gravitational Array*, “La Sapienza” preprint, Roma 1994.
- [20] Lobo J.A. and Ortega J.A., in *Proceedings of the First Edoardo Amaldi Meeting* (Frascati 1994), to appear.
- [21] I take this denomination from reference [9] above. It is, apparently, less common in the classical literature than the term *toroidal* applied to the other modes.
- [22] Eardley D.M., Lee D.L. and Lightman A.P., *Phys Rev* **D8**, 3308 (1973).
- [23] Astone P., Lobo J.A. and Schutz B.F., *Class Quan Grav* **11**, 2093 (1994).
- [24] Helstrom C.W., *Statistical Theory of Signal Detection*, Pergamon 1968.
- [25] Landau L.D. and Lifshitz E.M., *The Classical Theory of Fields*, Pergamon 1985.
- [26] Barut A.O., *Electrodynamics and Classical Theory of Fields and Particles*, Dover 1980.
- [27] Brans C. and Dicke R. H., *Phys. Rev.* **124**, 925 (1961)
- [28] Lobo J.A., unpublished.
- [29] Love A.E.H., *A Treatise on the Mathematical Theory of Elasticity*, Dover 1944.
- [30] Abramowitz M. and Stegun I.A., *Handbook of Mathematical Functions*, Dover 1972.

## List of Figures

**Figure 1** The homogeneous sphere *spheroidal* eigenvalues for a few *multipole* families. Only the  $l=0$  and  $l=2$  families couple to metric GWs, so the rest are given for completeness and non-directly-GW uses. Note that there are *fewer* monopole than any other  $l$ -pole modes. The lowest frequency is the first *quadrupole*. The diagramme corresponds to a sphere with Poisson ratio  $\sigma=0.33$ . Frequencies can be obtained from the plotted values through equation (B6) for any specific case.

**Figure 2** The homogeneous sphere *toroidal* eigenvalues. None of these couple to GWs, but knowledge of them can be useful for *vetoing* purposes. These eigenvalues are *independent* of the material's Poisson ratio. To obtain actual frequencies from plotted values, use (B6). The lowest *toroidal* eigenvalue is  $kR = 2.5011$ , with  $l=2$ , and happens to be the *absolute minimum* sphere's eigenvalue. Compared to the *spheroidal*  $kR = 2.6497$ , also with  $l=2$ , its frequency is 5.61% smaller. Note also that there are no monopole toroidal modes.

**Figure 3** First three *spheroidal monopole* radial functions  $A_{n0}(r)$  ( $n = 1, 2, 3$ ), equation (B19a).

**Figure 4** First three *spheroidal quadrupole* radial functions  $A_{n2}(r)$  (continuous line) and  $B_{n2}(r)$  (broken line) ( $n = 1, 2, 3$ ), equations (B19).

**Figure 5** First three *toroidal quadrupole* radial functions  $T_{n2}(r)$  ( $n = 1, 2, 3$ ), equation (B16). A common feature to these radial functions (also in the two previous Figures) is that they present a *nodal* point at the origin ( $r = 0$ ), while the sphere's surface ( $r/R = 1$ ) has a non-zero amplitude value, which is largest (in absolute value) for the lowest  $n$  in each group.

**Figure 6** The *scalar* component  $\mathbf{Z}^{(S)}(\mathbf{x}, \omega)$  of the *multimode* transfer function, (4.2a). The diagramme actually displays  $\omega^3 \mathbf{Z}^{(S)}(\mathbf{x}, \omega)$ , so asymptotic behaviours are better appreciated. It is given in units of  $\mu/\rho R$ , and a factor  $(\pi/i) \mathbf{u}_{n00}(\mathbf{x})$ , the eigenmode amplitude, has been omitted, too.  $\delta$ -function amplitudes are symbolically taken as 1. Note that the asymptotic regime, given by equation (4.4), is quickly reached.

**Figure 7** The *quadrupole* component  $\mathbf{Z}^{(m)}(\mathbf{x}, \omega)$  of the *multimode* transfer function, (4.2b). The same prescriptions of Figure 6 apply here; the plot is therefore *independent* of the value of  $m$ . Note the presence of *three* subfamilies of peaks; asymptotic regimes are reached with variable speed for these subfamilies, and less rapidly than for monopole modes, anyway.

*Spheroidal spectrum*

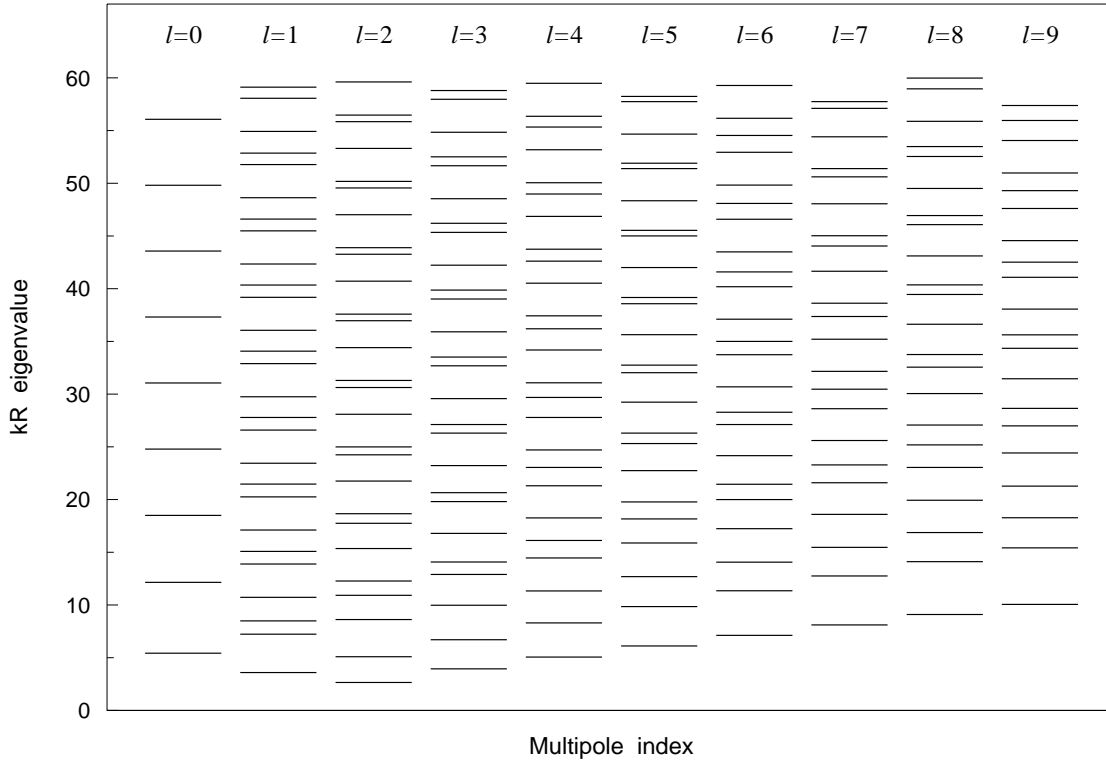


**FIG. I**

*Toroidal spectrum*

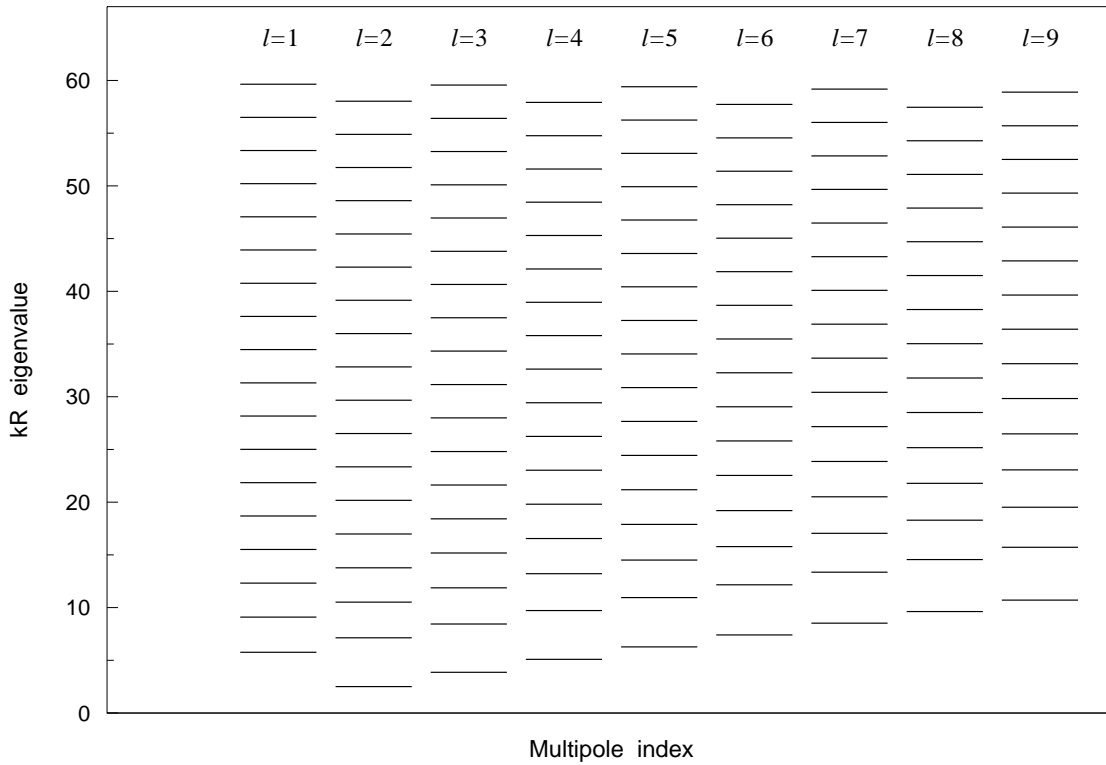


**FIG. II**

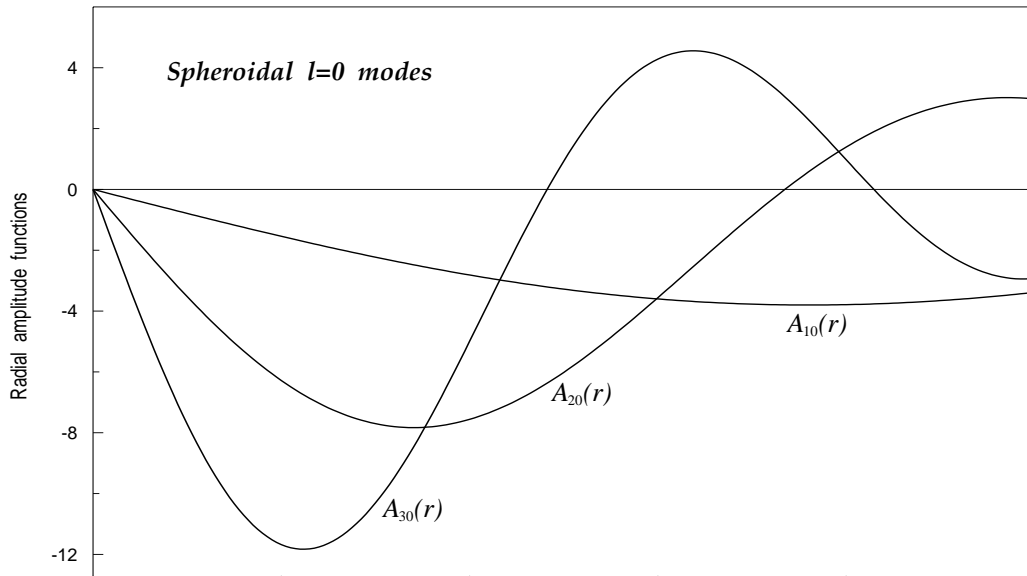


FIG. III

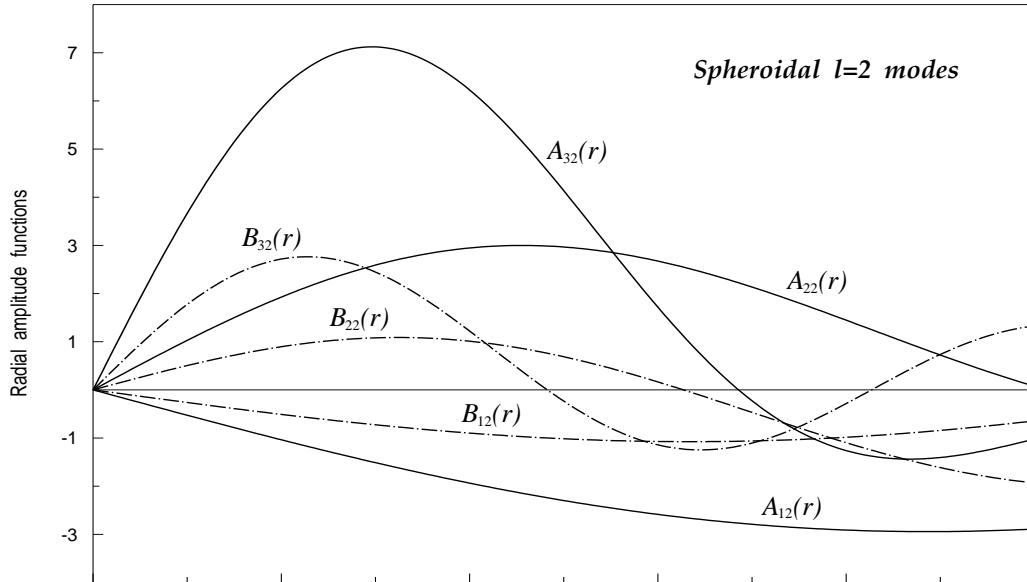


FIG. IV

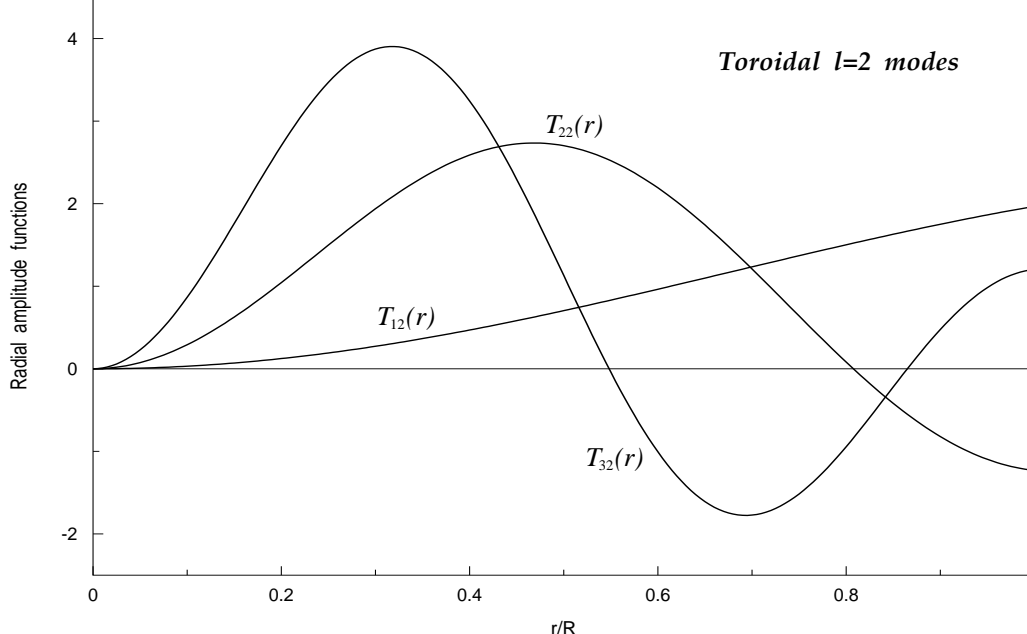
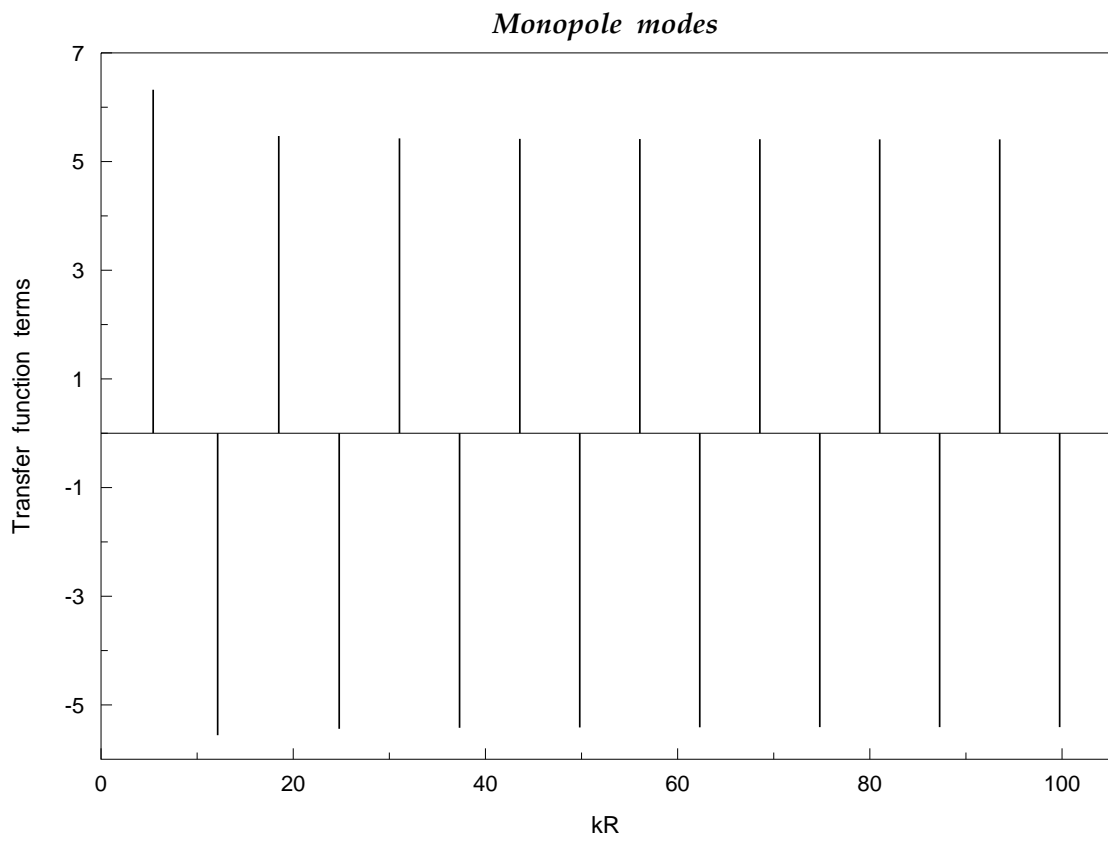
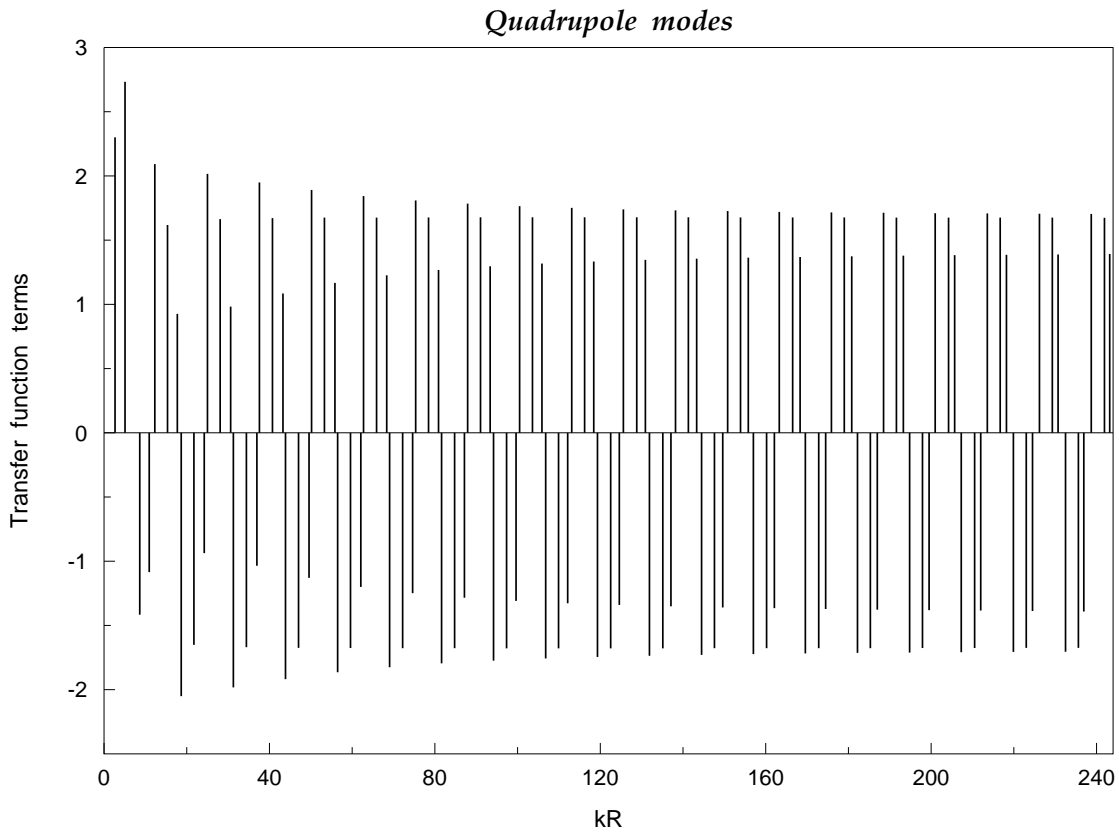


FIG. V



**FIG. VI**



**FIG. VII**